Cirrus Classification at Midlatitude from Systematic Lidar Observations

Philippe Keckhut, François Borchi, Slimane Bekki, Alain Hauchecorne, M. Silaouina

Cirrus Classification at Midlatitude from Systematic Lidar Observations

P. KECKHUT, F. BORCHI, S. BEKKI, A. HAUCHECORNE, AND M. SILAOUINA

Service d'Aéronomie/Institut Pierre-Simon Laplace, CNRS, Verrières le Buisson, France

(Manuscript received 29 December 2004, in final form 5 June 2005)

ABSTRACT

Systematic cirrus lidar measurements performed in the south of France during 2000 are analyzed statistically to search for cloud classes. The classes are based on cloud characteristics (cloud thickness, light backscattering efficiency, and its variance), cloud absolute geometric height, cloud height relative to the tropopause, and the temperature at the cloud level. The successive use of principal component analysis, cluster methods, and linear discriminant analysis allows the identification of four cirrus classes. Almost all the cirrus detections correspond to three classes with similar proportion of the total cirrus detected (around 30%). The absolute geometric height and the thickness are found to be the main discriminant variables. The first cirrus class corresponds to thin clouds above the local tropopause (absolute geometric height: 11.5 km), or at least around the tropopause, while another class corresponds also to thin clouds but at a lower altitude range in the troposphere (absolute geometric height: 8.6 km). The third class corresponds to thick clouds (thickness of 3.2 km) located below the tropopause, in an altitude range between the two first classes (absolute geometric height: 9.8 km). As expected, the high-altitude cirrus class is characterized with the lowest mean temperature. It is noted that the temperature is closely related to the altitude and so the role of temperature in the cirrus classes cannot be disentangled from the role of the altitude.

1. Introduction

Cirrus clouds are a major uncertainty in climate change assessments (Houghton et al. 2001). Despite many studies reporting cirrus observations, sometimes in conjunction with relevant parameters (temperature, humidity, aerosols, wind, waves, etc.), cirrus clouds are far from being extensively characterized, especially their vertical distribution. Moreover, the exact role of these different parameters in cirrus formation is not well known (Lohmann et al. 2004). As a result, cirrus parameterizations in numerical climate models are still rather crude.

The lack of vertical characterization partly originates from the small amount of observations that have the required properties: high vertical resolution and high sensitivity. For liquid clouds, classifications have been developed very early on, based on simple visual information. A range of morphological characteristics such as color, contrast, texture, geometrical form, or spatial extension has been used to determine different classes of liquid clouds over different altitude ranges (i.e., low, middle and high clouds). The classifications have proved to be useful in the identification of cloud formation processes and their parameterization in general circulation models. In contrast, cirrus clouds are usually described as being one class: ice clouds with no distinction according to the altitude. Most of the cirrus clouds can only be observed visually when the sun is at low zenith angles. With their low detection limit, lidar measurements are sensitive to even optically thin cirrus layers. The comparison of visual and lidar detection has led to two classes of ice clouds being distinguished: visible and subvisible clouds (Sassen et al. 1989). Note that it has not been shown that these two classes represent cirrus clouds with fundamentally different morphologies or formation processes. There have been attempts to identify more cirrus clouds classes. For example, a classification method based on clustering has been applied to the three channels of the Meteosat imagery (Desbois et al. 1982). Six classes of clouds were identified according to their optical depth from thick to very thin clouds. Three classes corresponded to cirrus clouds.

It is important to point out that altitude range and vertical extension of cirrus clouds are critical param-

Corresponding author address: Philippe Keckhut, Service d'Aéronomie, BP 3, 91371 Verrières-le-Buisson, France.
E-mail: keckhut@aerov.jussieu.fr

eters for the radiative balance of the atmosphere. A cirrus cloud at high altitudes and, hence, a cold cloud, influences more strongly the infrared flux than the same cirrus at a lower altitude. In contrast, a cirrus cloud at low altitudes has a weaker effect on the overall infrared fluxes and therefore the albedo effect (cirrus cloud reflecting back to space the incoming solar radiation) may dominate. Lidar measurements provide accurate information on the vertical distribution of cirrus and, therefore, are now used to develop highly resolved cirrus databases. The first height-resolved cirrus climatology developed from midlatitude lidar data revealed a frequency of cirrus occurrence of nearly 50% all yearround (Goldfarb et al. 2001). This is consistent with visual investigations performed on board aircraft (Clodman 1957). Lidar observations give access to several cirrus characteristics such as the cloud absolute geometric height, cloud thickness, backscattering ratio (called here intensity, which is related to the number of particles, their size, and their mean backscattering efficiencies), and its temporal variability (related to the horizontal structures because cirrus usually are not stationary structures). From this set of parameters combined with auxiliary data, one can attempt to identify different classes of cirrus. This type of classification could be useful for the validation of height-resolved cirrus fields calculated by models. It would complement actual model validations that are based on vertically integrated quantities such as cloud cover and infrared radiation fluxes measured from space. In addition, in the same way as liquid cloud classifications, cirrus classifications could provide clues on the key processes controlling cirrus formation and evolution.

In this study, a statistical multivariate analysis of one year of lidar data acquired in the south of France is carried out in order to determine whether distinct classes of cirrus can be identified. In a first section, the lidar and auxiliary data are described. In the second section, statistical methods are briefly presented and then the results are reported. In the last section, the characteristics of the different classes of cirrus are discussed and conclusions drawn.

2. Data description

Data consist mainly of systematic lidar data that have been obtained at middle latitudes in the south of France. Temperature profiles from a nearby radiosonde station complement the lidar data. Also, because cirrus are formed in the vicinity of the tropopause, their position with respect to the dynamical tropopause is derived from high-resolution potential vorticity (PV) fields produced by a PV advection model.

a. Lidar measurement at OHP

Cirrus clouds have been systematically measured for several years with a lidar in the south of France at the Observatoire of Haute-Provence (OHP; 44°N, 6°E). Measurements are conducted in a semiautomatic mode, during several hours at night, depending on the weather conditions (the lidar system does not operate when low clouds or rain are present). The temporal resolution of the measurements is 3 min and the vertical resolution is 75 m. Parameters such as the mean altitude of the cloud layer are usually averaged over longer time periods. Cirrus detected above OHP from 1997 and 1999 have already been studied, and a first climatology of their main characteristics (height, thickness, and mean backscattering ratio) has been published (Goldfarb et al. 2001). About 23% of the observations were found to be subvisible cirrus clouds, according to the criteria of Sassen et al. (1989).

The algorithm of cirrus detection used in the present study is based on fitting the background scattering and then estimating the scattering enhancement resulting from ice particles. A constant lidar ratio of 18 sr^{-1} (Platt and Dilley 1984) is used in the retrieval algorithm. This method of cloud retrieval is more sensitive to sharp enhancement than to diffuse background aerosols changes. Therefore, it is well suited to the detection of cirrus clouds. Nonetheless, because no information on the composition of the scattering layer can be derived directly with one wavelength lidar, thin particle layers (e.g., of volcanic origin) could be interpreted as a cloud. During the period investigated, no major volcanic eruptions have been reported (see information online at http://toms.umbc.edu). Therefore, the scattering particles in the upper troposphere–lower stratosphere (UTLS) are most probably composed of ice, at least partly, and so are treated as cirrus here. The lidar system and the detection algorithm have already been described in details in (Goldfarb et al. 2001). A quite low detection level is achieved because measurements are conducted at night with a small field of view. From these measurements, several macroscopic parameters associated with the vertical distribution of the clouds, their optical properties, and temporal variability can be derived. Cloud parameters are estimated over 3-min measurement periods and then averaged over several hours except when there was a change in meteorological conditions during the averaging period. The selected parameters are described hereinafter:

1) The absolute geometric height of the cloud is provided with a resolution of 75 m. The geometric height is deduced from the top and bottom height of the cloud.

2) The thickness of the cloud is the mean difference between the top and the base of the cloud. Because cirrus appears as thin, intense enhancements of the lidar signal, this parameter can be accurately derived (within the vertical resolution of 75 m). The optical depth can be deduced from the thickness and the mean backscattering ratio, assuming the backscattering is constant within the cloud. Because the lidar ratio is assumed to be constant within the cloud, the optical depth cannot be accurately derived and hence is not used as a cloud parameter in the search for a classification. However, cloud climatologies derived from lidar data often refer to the optical depth. Therefore, it might be valuable to estimate the optical depth for each cloud and derive a mean value for each cloud class.
3) The backscatter is the parameter measured by lidars; the mean backscattering ratio is usually defined as the ratio of aerosol scattering to the total backscattering. In our case, the ratio is defined as the ratio of the cirrus backscattering (excluding background aerosol contribution) to the total backscattering. It is called intensity in the following. This parameter is related to the particle scattering efficiency and particle number density.

Like liquid water clouds, horizontal patterns in cirrus clouds (Conover 1960; Sassen et al. 1990) partly originate from the cloud formation and evolution. The temporal variability (which is linked to the spatial variability) of a cirrus cloud is quantified here with the standard deviation of the mean backscattering ratio over the successive 3-min measurement records. Because the amplitude of the standard deviation is strongly related to the amplitude of the mean backscattering, we have considered the ratio of these two quantities (i.e., scaled standard deviation). Some sensitivity tests have shown that the variability parameter could be discarded from the final classification analysis because it was found to play a very minor role in the cirrus classification.

b. Radiosonde data

Temperature is a key parameter in cloud formation. Radiosondes are regularly launched by the French meteorological center (Meteo-France) at Nimes, a site close to OHP (110 km westward). The systematic soundings at midnight, during the lidar operation, allow us to estimate the mean temperature at the cloud level. Although the temperature measurements exhibit some variability, the temperature field is supposed to be relatively uniform within few kelvin between Nimes and OHP.

The water vapor is also a critical parameter in cloud formation. However, the accuracy of humidity measurements with standard radiosondes is rather poor in the upper troposphere. For this reason, these data are discarded from the analysis.

c. MIMOSA

In addition to the issue of the altitude range of cirrus clouds and of their radiative impact, the position of cirrus clouds with respect to the tropopause is important. Indeed, it is highly relevant to the issue of heterogeneous chemistry and the associated lower-stratospheric ozone depletion (Solomon et al. 1997). Troposphere and stratosphere exhibit radically different properties in terms, for example, of static stability or chemical composition. The altitude of the tropopause used in our analysis is based on static stability and relates to the altitude of 1.6 PV unit (PVU) level (WMO 1986). It is called the dynamical tropopause. In contrast to temperature fields, PV fields are highly structured around the tropopause. To take into account this spatiotemporal variability, PV profiles above OHP are derived using a three-dimensional high-resolution PV advection model called Modèle Isentropique de Transport Méso-échelle de l'Ozone Stratopshérique par Advection (MIMOSA). MIMOSA uses the potential temperature as the vertical coordinate. In the present case, the model is run on an elementary horizontal grid of 37 km $\times$ 37 km (three grid points per degree of latitude) and is forced with winds from 6-h European Centre for Medium-Range Weather Forecasts (ECMWF) analyses of 1.125° latitude $\times$ 1.125° longitude resolution, corresponding to a T106 truncation (Hauchecorne et al. 2002). On the time scale of a few days, PV can be considered as a quasi-passive tracer in regions where turbulence and convection are weak, typically in the stratosphere and, to a lesser extent, around the tropopause. The PV fields on an isentropic (constant potential temperature) surface are calculated by advecting PV and relaxing it toward PV values from ECMWF analyses with a time constant of 10 days. The ability of MIMOSA to describe small-scale structures through the advection of PV as a quasi-passive tracer has already been evaluated in the UTLS (Hauchecorne et al. 2002; Heese et al. 2001). An example of a longitudinal distortion of PV contours on an isentropic surface is shown is in Fig. 1. Typical PV profiles above OHP exhibit small values (around or smaller than 1 PVU) for potential temperature below around 330 K (approximately 12 km) and then, because of the static stability of the stratosphere, increase rapidly, reaching values around 8 PVU at 400 K (16 km). The potential temperature of the local dynamical tropopause is defined here as the level corresponding to the 1.6-PVU thresh-

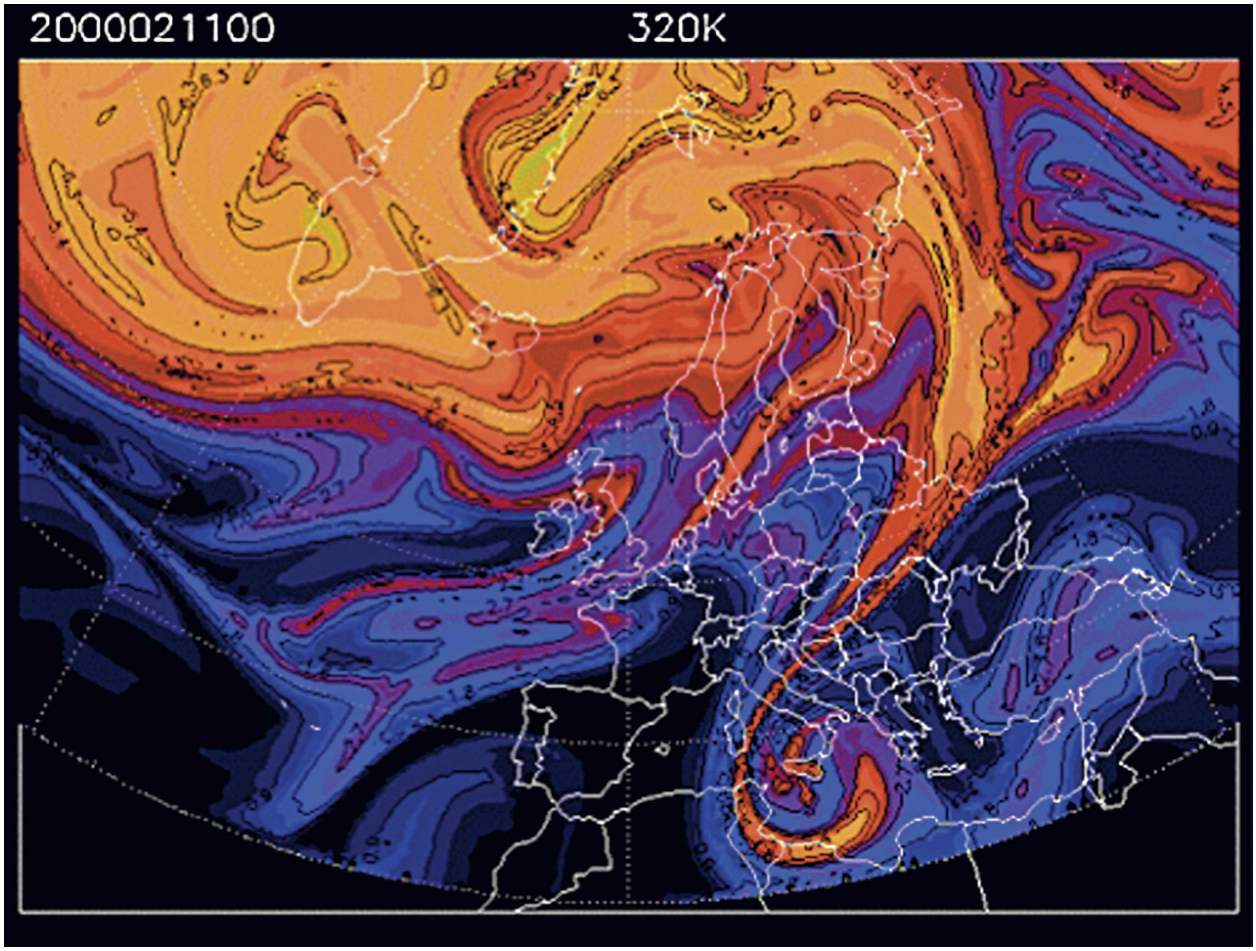

FIG. 1. An example of the advected PV field calculated by MIMOSA for the 320-K isentropic level on 11 Feb 2000. Blue colors correspond to PVUs around 2 and can be viewed as the region of the dynamical tropopause. One can notice a thin structure of stratospheric air over central Europe.

old value (WMO 1986). The geometric heights of clouds are converted into potential temperature levels using the radiosonde measurements and then compared with the tropopause level. The difference between these altitudes is one of the parameters used in the classification analysis and is called the relative altitude.

3. Methodology of multivariate analyses

Before performing a complex multivariate analysis (MA), we first start by studying the probability distribution of the variables in our data sample in order to see whether cirrus classes could already be identified. The probability distribution functions (PDFs) of different observed variables are not Gaussian (Fig. 2). There are indications of possible different classes in the broad features of the PDFs. For example, the PDF of the mean cirrus suggests several modes exhibiting two maxima centered at 8.5 and 11.5 km. The same feature is found for the thickness of the cirrus with one group centered at 1 km and another group centered at 3 km. On the PDF of the temperature, there is one very large mode centered at −45°C approximately and a small mode at −60°C. However, visual analysis can be deceptive, and any conclusions from these PDFs can be tainted with subjectivity. In addition, cirrus groups end up being defined from one parameter at a time. To avoid the use of any visual analysis and to take into account the cross correlations (correlation between parameters) explicitly in the cirrus classification, thorough multivariate analyses are carried out. The multivariate approach should be more efficient and objective for deciding whether different clusters can be identified and discriminated using the available data. In the rest of this section, principal component analysis (PCA), cluster methods (CMs) and linear discriminant analysis (LDA) are briefly described. Data reduction by PCA is achieved by finding linear combinations (principal com-

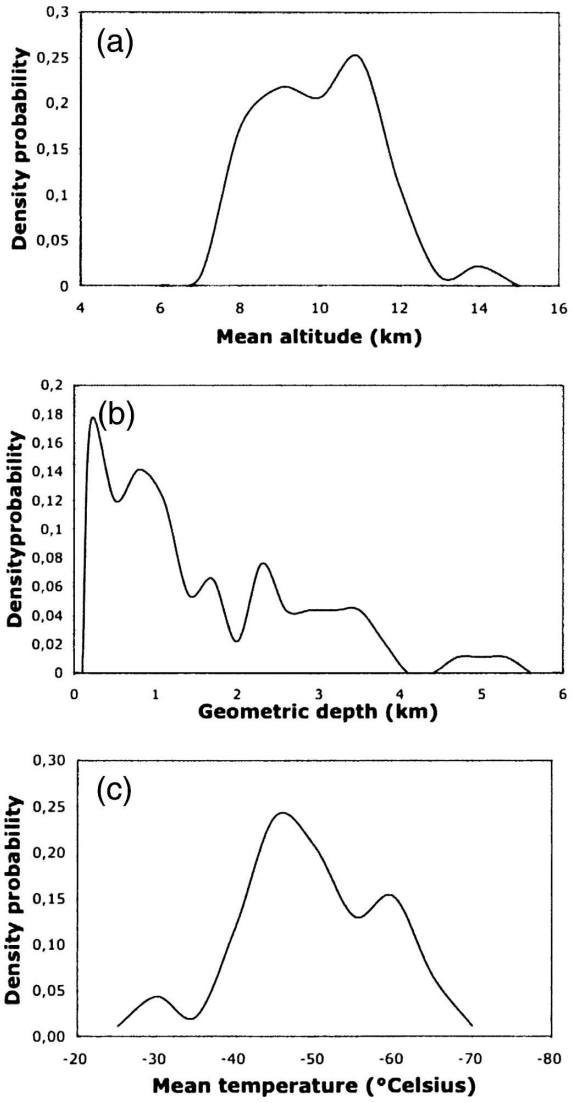

FIG. 2. Histogram of probability distribution for three observed variables: (a) absolute geometric altitude, (b) thickness, and (c) mean temperature of the cirrus clouds.

ponents) of the original variables, which account for as much as possible of the original total variance (Jolliffe 1986). PCA is performed to create new uncorrelated variables and reduce the data dimension. It also helps in identifying meaningful features in data on a graphical representation (with principal axes). The aim of CM is to group data into clusters or classes usually using algorithms that maximize distances between clusters in the variable space and minimize distances between data belonging to the same clusters (Anderberg 1973). We use two different types of CM—hierarchical clustering methods (HCM) according to the Ward's method and the *K*-means clustering (KMC). The aim of HCM is to calculate the distance between data entries and to agglomerate. The result is a hierarchical tree in which the clusters (agglomerate of observations) are organized based on growing distances. Hierarchical methods require so much computer storage that nonhierarchical methods such as the KMC methods are usually preferred. MacQueen (1967) used the term "*K* means" for a process where each data unit (each observation) is assigned to that element of a set of *K* clusters that has the nearest centroid (mean). The aim is to cluster the data in order to minimize the sum of the inner distances and to have a reasonable number of clusters. Last, LDA are multivariate analyses used to classify or reclassify data into two or more groups in a quantitative manner (Cacoullos 1973). An attempt is made to interpret the physical meaning of the resulting classification with respect to the original variables. LDA produces a small number of linear functions useful for discriminating among clusters of data obtained previously, for example, with a CM. From the discriminant linear functions, data membership probabilities to clusters can be calculated, allowing data to be reclassified after LDA. Overall, LDA provides the mean to validate and optimize results from cluster methods, and to determine the cluster of additional observations. Moreover, the discrimination power for each original variable is estimated with LDA.

The discrimination between cirrus clouds detected above OHP relies on the successive application of the following multivariate analyses: 1) PCA with absolute and relative height, thickness, intensity, and temperature of cirrus clouds; 2) HCM as Ward's technique on the first PCs to determine the exact number of cirrus classes; 3) KMC to compare with the results obtained with HCM; 4) LDA to optimize the classification produced with HCM or KMC until 0% of classification error is obtained. More details about this methodology can be found in Borchi and Marenco (2002) where the same approach has been used successfully on UTLS data. Multivariate analyses are performed with the XLSTAT software (version 4b).

4. Results of multivariate analyses

a. Principal component analysis

Ninety-two cirrus clouds were detected above OHP in 2000. The data matrix for the 92 observations (Fig. 3) consists of 92 rows (data = detected cirrus) and five columns (variables = absolute and relative height, thickness, intensity, and temperature). The first PC accounts for 44% of the total variance, while the second component account for 23%, the third for 18%, the fourth for 12%, and the fifth for 3%. The correlation circle shown in Fig. 3 is a synthesis of the correlation

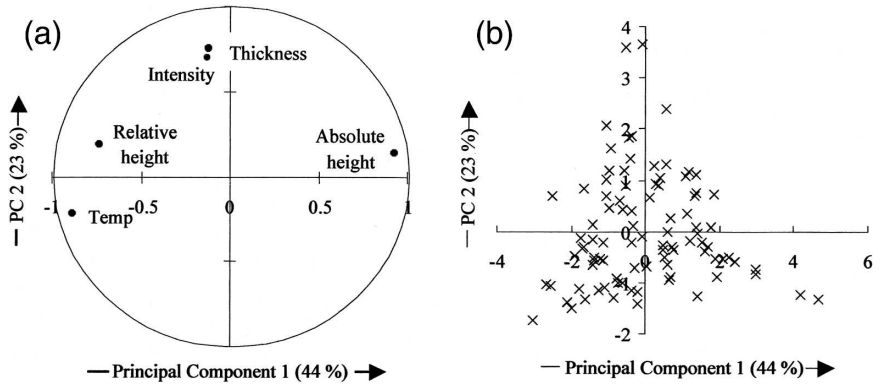

FIG. 3. (a) Correlation circle and (b) scatterplot of the first two PCs for the 92 cirrus cloud systems detected in 2000. PC1 for (a) and (b) are not exactly the same, but they are linearly correlated.

matrix and of the correlations between initial variables and PCs.

When analyzing the PCA results, one has to keep in mind that the original variables are not independent. Some variables show high levels of correlation. For example, as expected, absolute height and temperature are both very strongly anticorrelated with $r = -0.81$. The absolute height is strongly correlated with the first PC ($r = 0.92$), whereas the temperature is anticorrelated with it ($r = -0.88$). The relative height is anticorrelated with the first PC ($r = -0.74$). The first PC appears to be a measure of cirrus according to increasing values of absolute height and decreasing values of temperature and relative height. Thickness and intensity are correlated with the second PC with $r = 0.75$ and $r = 0.7$, respectively. Intensity is also correlated with the third PC ($r = 0.7$). The five variables are rather well represented by the first two PCs. Indeed, the projection of variables on the factor plan is close to the circle. The scatterplot for the first two PCs (data projection on the first two PCs plan) shown in Fig. 3b provides a graphical representation of the distribution of the data points. All of the data points near the right part of PC 1 correspond to low values of relative height and temperature (temperature is relative so negative values) and high values of absolute height, and therefore are characteristic of the highest cirrus clouds (around the tropopause). The group of points, near the left-hand side of PC 1, corresponds to the lowest cirrus. Data points near the upper (and conversely lower) part of PC 2, represent cirrus with high (and conversely low) values of thickness and intensity. The left-hand lower quadrant (with negative values of PC 1 and PC 2) corresponds to cirrus with low values of absolute height, thickness, and intensity, and high values of relative height and temperature. Theses results suggest that some grouping of the cirrus data points might be possible. But, do these groups correspond to real and homogenous classes of cirrus with distinct characteristics? And what is the cluster for each observation and what is the exact number of clusters? Cluster methods as HCM and KMC can help to answer to those questions.

b. *Cluster methods*

The use of the first three PCs (with 90% of points having a good projection on the first three PCs) in cluster methods instead of the original data allows the noise in the data to be fit corresponding to the fourth and fifth principal components (with, respectively, only 12% and 3% of the total variance), resulting in a better classification. The advantage of HCM is that the hierarchical tree provides the optimum number of clusters. The breaking of the level index between 88 and 89 nodes (for a total of 92 observations) shows that the processing of the data as by HCM gives four clusters (not shown).

We also apply a different cluster method, KMC, in order to check the robustness of the classification obtained with HCM. KMC leads to results similar to HCM with four clusters and only five different cluster affectations on 92 observations.

c. *Linear discriminant analysis*

LDA is used after the cluster methods to validate and optimize the clustering and to estimate the discrimination power of each variable. The same data matrix as for PCA is used in discriminant analysis (DA), but it also includes a variable containing the clusters obtained with HCM. The clusters obtained with KMC are also tested. Note that DA provides an estimate of the error percentage on the classification: around 4% with clus-

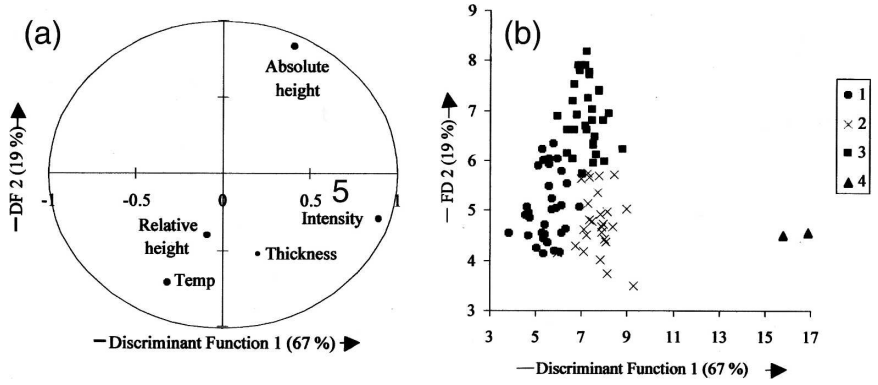

FIG. 4. (a) Discrimination circle and (b) scatterplot of the first two discriminate functions for the 92 cirrus cloud systems detected in 2000. DF1 for (a) and (b) are not exactly the same, but they are linearly correlated.

ters from HCM and 4% for the clusters from KMC, validating the cluster analysis. Also, DA provides a new refined reclassification. The process can be further optimized by applying DA to the new classification. It can be done as many times as necessary until 0% of classification error is obtained. The final LDA results shown on Figs. 4 and 5 are quite similar to those obtained with PCA, but with linear discriminant functions instead of principal components. The first discriminant function is very strongly correlated to intensity ($r = 0.9$) and has a discrimination power of 67% (see Fig. 4a). So, the most discriminating variable is the intensity. The second discriminant function is very well correlated to absolute height ($r = 0.83$) and anticorrelated to temperature ($r = -0.72$), and has a discrimination power of 19% (see Fig. 4a). The third is very well correlated to the thickness ($r = 0.80$) and has a discrimination power of 14% (see Fig. 5a). The relative height is not a discriminating variable (no correlation with the discriminant functions). The function values (see Figs. 4b and 5b) show a good discrimination between these four cirrus classes. For example, the cirrus class 2 corresponds to a cirrus group with high values of intensity, temperature (temperature in negative values), and thickness, and low values of absolute height. The optimization of the classification with DA after HCM or KMC gives practically the same cirrus classes.

5. Discussions and conclusions

The principal component analysis indicates that they are patterns in the large cloud of 92 data points plotted as a function of five variables (absolute and relative height, thickness, intensity and temperature of cirrus) space. Clearly, there is strong correlation between some variables. The use of the first principal components in cluster methods rather than the initial data reduced the influence of the noise in the classification analysis. HCM and KMC lead to practically the same clusters, showing the robustness and consistency of these two

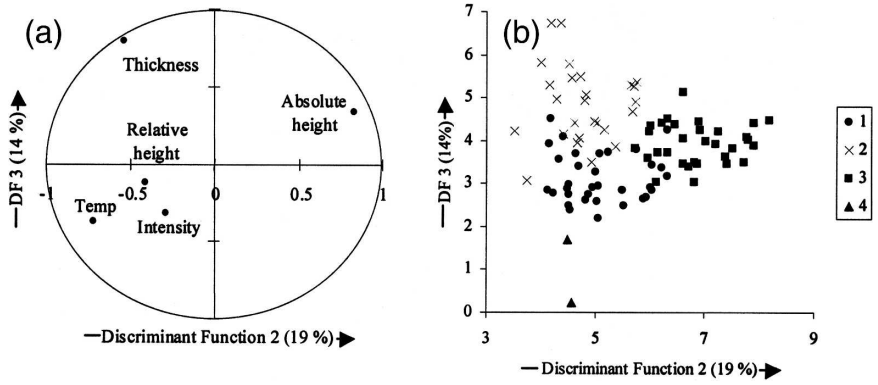

FIG. 5. (a) Discrimination circle and (b) scatterplot of the second and third discriminate functions for the 92 cirrus cloud systems detected in 2000.

cluster methods. To optimize the cluster analysis, LDA is applied several times to the HCM and KMC results until 0% of classification error is obtained. The mean and standard deviation for all the parameters of each cirrus class are listed in Table 1, including the optical depth and the temporal variability, even if they were not used in the determination of the classification.

The mean value of the parameter associated with the temporal variability of cirrus is very similar for all the classes. It is a bit surprising because it should contain useful information for discriminating cirrus based on their horizontal structures (linked to temporal variability in the scattering ratio). Nonetheless, there are a number of reasons for this similarity in the temporal variability for all the cirrus classes. First, the temporal standard deviation corresponds to deviations from the mean during the time interval of measurements, several hours typically, without any information about the frequency components of the temporal variations (which are somewhat related to spatial variations because the cirrus are not stationary structures usually). Second, the temporal standard deviation is calculated from data obtained when cirrus are detected (i.e., signal enhancement above a certain threshold). In the case of broken clouds, the time intervals without cloud detection are discarded. As a result, the real variability parameter is not properly estimated. This probably explains partly why the mean temporal standard deviation does not vary much from one cirrus class to another.

The frequencies of occurrence are comparable for the first three cirrus classes whereas the cirrus clouds from the last class are rare. This last class (episodic highly scattering cirrus) is based on two cases only that were exceptional in terms of intensity (mean backscattering ratio). However, this class is close to the second and third class regarding the altitude and similar to the third class in terms of thickness and optical depth. Further investigations on a larger data sample will be required to see whether these cirrus can be considered a distinct class.

The second class (thick upper troposphere cirrus) corresponds to cirrus presenting large optical depths. This cirrus exhibits the largest thickness (3.2 km) and are located just below the local tropopause. The top altitude is usually defined by the local tropopause height. By contrast, the first class (midtroposphere thin cirrus) corresponds to thin cirrus clouds (1 km) that are located at the lowest altitudes, on average at 8.6 km. The corresponding mean temperature inside the cloud is equal to −41°C. The third class (thin tropopause cirrus) corresponds to very similar clouds, except that they are located at higher altitudes. They seem to be slightly above the local tropopause on average. The amplitude of the standard deviation reveals a large dispersion of the cloud position relative to the tropopause. Those clouds may be related to cumulonimbus clouds anvils advected to midlatitudes (Garrett et al. 2004) or to moist air masses transported isentropically from the tropical upper troposphere into the lowermost stratosphere. A statistical study based on ECMWF analyses shows that such transport of moist air from tropical regions into the stratosphere is relatively frequent with a transit time of several days (Fueglistaler et al. 2004). A more thorough analysis is required for proving unambiguously that they are located into the stratosphere.

The cirrus classification reflects largely the broad features seen in the probability distributions (see Fig. 1). The first maximum at about 9 km in the mean cirrus height PDF corresponds clearly to class I (8.6 km), whereas the second maximum at 11 km is a convolution of classes II and III that are centered at 9.8 and 11.5 km, respectively. In the same way, the first large group centered at about 1 km in the cloud thickness PDF corresponds to classes I and III (0.9 km) while the second group between 2 and 4 km could correspond to class II. Last, the maximum at −45°C in the cloud temperature PDF corresponds to a convolution of the distributions of classes I and II. The secondary maximum at around −60°C corresponds to class III.

A previous classification based on Meteosat images

TABLE 1. Characteristics of the four cirrus classes.

Class type	I: Midtroposphere thin cirrus	II: Thick upper troposphere cirrus	III: Thin tropopause cirrus	IV: Episodic highly scattering cirrus
Occurrence (%)	36	27	35	2
Geometric height (km)	8.6 ± 0.9	9.8 ± 0.7	11.5 ± 0.9	10.6 ± 0.3
Thickness (km)	0.9 ± 0.6	3.2 ± 0.9	0.9 ± 0.6	1.0 ± 0.8
Intensity of the mean backscattering ratio	8.2 ± 4.8	12.9 ± 5.3	8.4 ± 4.2	72 ± 7
Standard deviation of the backscattering ratio	0.7 ± 0.3	0.9 ± 0.3	0.7 ± 0.4	0.9 ± 0.1
Relative height (differential potential temperature in kelvin)	7 ± 8	0.5 ± 13	−7 ± 16	4.2 ± 3.5
Mean temperature inside the cloud (°C)	−41 ± 6	−50 ± 6	−58 ± 6	−49 ± 0.9
Estimated optical depth	0.2 ± 0.2	0.8 ± 0.4	0.13 ± 0.1	1.3 ± 1

(Desbois et al. 1982) reported three classes associated with thick, thin and very thin cirrus. This classification is not in contradiction with the present analysis. In addition, our results provide useful complementary information associated with the vertical cloud structure.

It is difficult to conclude from these results whether the temperature has an effective role in discriminating among cirrus types because temperature in the troposphere is highly correlated with altitude. A recent study of depolarization ratio by Noel et al. (2002) has shown different cirrus classes based on the shape ratio of the particles when cirrus are assumed to be hexagonal crystals. Noel et al. inferred four cirrus classes on a comparable dataset obtained with a lidar located in the vicinity of Paris, about 500 km northward of OHP. In their study, one class was associated with low temperature (mean temperature centered around −58°C) while the other classes exhibited a similar temperature distribution picking at −45°C. Their results are consistent with our findings. They also detected on two occasions thin (1 km) cirrus clouds located at high altitudes (11–12 km) that were very similar to the cirrus clouds of class III (thin tropopause cirrus). According to the authors, the cirrus clouds corresponded to crystals with long hexagonal columns of a shape ratio between 1.1 and 4, whereas the other classes exhibited a wide distribution of polarization inside the clouds that may indicate the presence of mixed-phased crystals.

Because cirrus clouds are the product of injection and freezing of water vapor into the dry and cold upper troposphere, it is expected that local cloud properties depend on weather processes and systems. A cirrus climatology has been developed from lidar data collected at midlatitudes in Utah (Sassen and Campbell 2001). They derived mean morphological parameters of cirrus clouds that are very similar to those of our study. They found a strong seasonal cycle that is not observed at OHP (located in Europe, 44°N latitude), probably because of the differences in prevailing weather systems. The authors did not identify cirrus classes. However, they presented an attempt to relate cirrus detection to different weather patterns. They identified tree major situations: zonal jet streamflow, strong amplitude ridge and cases of split-jet flow. This link between weather patterns and cirrus is not surprising because weather patterns determine to a large extent the variations in temperature, pressure and water vapor content in air masses where clouds can subsequently form. The cooling rate of air masses where cirrus clouds are observed is acknowledged to be a critical parameter (Karcher and Strom 2003), which is not accounted for in our analysis. Subsequent work could be to search for some relationship between weather patterns (critical for vertical velocity and hence cooling rate), morphological parameters, and, possibly, processes of cirrus formation. Note that, although this classification is representative of midlatitude cirrus, one can attempt to compare the results with cirrus studies at tropical sites. The annual cycle at our site appears to be very different from the one observed at subtropical sites (Cadet et al. 2003). In addition, only two classes of cirrus were identified from data obtained at a tropical site (Comstock et al. 2002). Nonetheless, the best way to compare the different sets of results would be to analyze tropical and subtropical cirrus datasets with an approach similar to the one described here.

It is worth pointing out that this type of height-resolved cirrus classification should prove useful in evaluating cloud models and hence help to improve parameterizations of cirrus in large-scale models because multiple processes may need to be considered. Even though the physical mechanisms that are responsible for generating the four phenomenological cloud classes remain uncertain, the analysis points toward the need to increase the vertical resolution of global models in order to better resolve different cloud layers and thus their radiative impact. Last, the depolarization ratio could be a very good discriminating parameter for cirrus classification because it provides information on the shape of the cirrus crystals (Noel et al. 2002). It would be valuable to add the depolarization as a cloud parameter in the classification analysis. Depolarization measurements are being planned at the OHP lidar site.

Acknowledgments. The authors acknowledge the OHP team for their continuous efforts of collecting the data of high quality and Leah Goldfarb for her contribution in lidar data handling. This work was performed in the framework of the French Programme Atmosphere et Océan Multi-échelles (PATOM); MONUMEEP. This work has been supported by the Environment and Climate Research Program of the European Commission under Contract EVK2-CT-2001-00112 (PARTS) and by the ADEME under Contract 0362C0075.

REFERENCES

Anderberg, M. R., 1973: *Cluster Analysis for Applications*. Academic Press, 359 pp.

Borchi, F., and A. Marenco, 2002: Discrimination of air masses near the extratropical tropopause by multivariate analyses from MOZAIC data. *Atmos. Environ.,* **36,** 1123–1135.

Cacoullos, T., 1973: *Discriminant Analysis and Applications*. Academic Press, 434 pp.

Cadet, B., L. Goldfarb, D. Faduilhe, S. Baldy, V. Giraud, P. Keckhut, and A. Rechou, 2003: A sub-tropical cirrus cloud clima-

tology from Reunion Island (21°S, 66°E) lidar data set. *Geophys. Res. Lett.,* **30,** 1130, doi:10.1029/2002GL016342.

Clodman, J., 1957: Some statistical aspects of cirrus clouds. *Mon. Wea. Rev.,* **85,** 37–41.

Comstock, J. M., T. P. Ackerman, and G. G. Mace, 2002: Ground-based lidar and radar remote sensing of tropical cirrus clouds at Nauru Island: Cloud statistics and radiative impacts. *J. Geophys. Res.,* **107,** 4714, doi:10.1029/2002JD002203.

Conover, J. H., 1960: Cirrus patterns and related air motions near the jet stream as derived by photography. *J. Atmos. Sci.,* **17,** 532–546.

Desbois, M., G. Seze, and G. Szejwach, 1982: Automatic classification of clouds on METEOSAT imagery: Application to high-level clouds. *J. Appl. Meteor.,* **21,** 401–412.

Fueglistaler, S., H. Wernli, and T. Peter, 2004: Tropical troposphere-to-stratosphere transport inferred from trajectory calculations. *J. Geophys. Res.,* **109,** D03108, doi:10.1029/2003JD004069.

Garrett, T. J., A. J. Heymsfield, M. J. McGill, B. A. Ridley, D. G. Baumgardener, T. P. Bui, and C. R. Webster, 2004: Convective generation of cirrus near the tropopause. *J. Geophys. Res.,* **109,** D21203, doi:10.1029/2004JD004952.

Goldfarb, L., P. Keckhut, M.-L. Chanin, and A. Hauchecorne, 2001: Cirrus climatological results from lidar measurements at OHP (44°N. 6°E). *Geophys. Res. Lett.,* **28,** 1687–1690.

Hauchecorne, A., S. Godin, M. Marchand, B. Heese, and C. Souprayen, 2002: Quantification of the transport of chemical constituents from the polar vortex to middle latitudes in the lower stratosphere using the high-resolution advection model MIMOSA and effective diffusivity. *J. Geophys. Res.*, **107,** doi:10.1029/2001JD000491.

Heese, B., S. Godin, and A. Hauchecorne, 2001: Forecast and simulation of stratospheric ozone filaments: A validation of a high-rersolution potential vorticity advection model by airborne ozone lidar measurements in winter 1998/1999. *J. Geophys. Res.,* **106,** 20 011–20 024.

Houghton, J. T., Y. Ding, D. J. Griggs, M. Noguer, P. J. van der Linden, X. Dai, K. Maskell, and C. A. Johnson, Eds., 2001: *Climate Change 2001: The Scientific Basis*. Cambridge University Press, 892 pp.

Jolliffe, I. T., 1986: *Principal Component Analysis*. Springer, 502 pp.

Karcher, K., and J. Strom, 2003: The roles of dynamical variability and aerosols in cirrus cloud formation. *Atmos. Chem. Phys. Discuss.,* **3,** 1415–1451.

Lohmann, U., B. Kärcher, and J. Hendricks, 2004: Sensitivity studies of cirrus clouds formed by heterogeneous freezing in the ECHAM GCM. *J. Geophys. Res.,* **109,** doi:10.1029/2003JD004443.

MacQueen, J., 1967: Some methods for classification and analysis of multivariate observations. *Proceedings of the Fifth Berkeley Symposium of Mathematical Statistics and Probability,* Vol. 1, University of California Press, 281–297.

Noel, V., H. Chepfer, G. Ledanois, A. Delaval, and P. H. Flamant, 2002: Classification of particle shape ratios in cirrus clouds based on the lidar depolarization ratio. *Appl. Opt.,* **41,** 4245–4257.

Platt, C. M. R., and A. C. Dilley, 1984: Determination of the cirrus particle single-scattering phase function from lidar and solar radiometric data. *Appl. Opt.,* **23,** 380–386.

Sassen, K., and J. R. Campbell, 2001: A midlatitude cirrus cloud climatology from the facility for atmospheric remote sensing. Part I: Macrophysical and synoptic properties. *J. Atmos. Sci.,* **58,** 481–496.

——, M. K. Griffin, and G. C. Dodd, 1989: Optical scattering and microphysical properties of subvisible cirrus clouds, and climatic implications. *J. Appl. Meteor.,* **28,** 91–98.

——, C. J. Grund, J. D. Spinhirne, M. H. Hardesty, and J. M. Alvarez, 1990: The 27-28 October 1986 FIRE IFO cirrus case study: A five lidar overview of cloud structure and evolution. *Mon. Wea. Rev.,* **118,** 2288–2311.

Solomon, S., S. Borrmann, R. R. Garcia, R. Portmann, L. Thomason, L. R. Poole, D. Winker, and M. P. McCormick, 1997: Heterogeneous chlorine chemistry in the tropopause region. *J. Geophys. Res.,* **102,** 21 411–21 429.

WMO, 1986: Atmospheric ozone 1985. WMO Report No. 16.